A non-local probabilistic method for modelling of crack propagation

Elia Gironacci[1], Mohaddeseh Mousavi Nezhad[1], Mohammad Rezania[1], Giovanni Lancioni[2]

[1]Computational Mechanics, Civil Research Group, School of Engineering, University of Warwick, Coventry, CV4 7AL, UK

[2]Department of Civil Engineering and Architecture (DICEA), Polytechnic University of Marche (UNIVPM), Via Brecce Bianche, 60131, Ancona, Italy

ABSTRACT

Damage process in engineering systems is strongly affected by spatial heterogeneity and local discontinuities in the materials, which are significantly influencing the reliability and integrity of the systems. In this paper, we present a new stochastic approach as a tool for performing uncertainty quantification in simulating damage evolution in heterogeneous brittle materials. One of the advantages of the proposed method is its ability to capture the influence of uncertainty in the mechanical properties of whole simulation domain, not just the properties of the immediate neighbourhood around the crack tip, on direction of crack propagation. In fact, through this approach the direction of crack propagation at a specified point of localised damage can be probabilistically determined based on nonlocal mechanics theory, in which the influence of local discontinuities and weak points located at further distances from the crack tip, in addition to those located at the immediate neighbourhood of the local damage, are incorporated into the model. The reliability and performance of the methodology are examined through simulation of numerical examples and comparison with analytical results and experimental data. The case studies show how the crack initiation angle can be reasonably estimated with this methodology and how this approach provides realistic values of fracture toughness K_{IC} and fracture energy G_f.

Key Words: *stochastic crack initiation angle; fracture toughness; mixed-mode fracture; nonlocal approach; non-Gaussian random field*

1. Introduction

In recent years, many researchers have focused on the problem of modelling heterogeneous material systems containing discontinuities. Numerous methodologies for inclusion of heterogeneity in numerical frameworks for simulating material failure behaviour have been developed, which can be grouped into two main categories: multi-scale models and stochastic approaches.

Multi-scale methods have offered a significant progress in explicitly describing local heterogeneities [1]. In fact, for the heterogeneous materials, like concrete, rocks or composites, often a local fine-scale definition of micro-structure of the materials that influence their macroscopic mechanical response is needed [2]. Developed understanding of multiple phase concepts is used in multi-scale techniques, where it is aimed to predict the joint multi-phase response of structures. Although multi-scale modelling has been proved to be a powerful method for incorporation of the heterogeneity, difficulties may arise when a detailed knowledge of the material micro-structure for identifying the representative elementary volume, is not available. For this reason, an increasing interest has now been directed towards stochastic approaches, as they allow probabilistic estimation of degree of heterogeneity in the materials by quantifying fluctuations of mechanical properties [3-6, 46].

The two main processes for brittle failure of materials are crack initiation and crack propagation. From a physical point of view, when a body is deformed, the corresponding stored strain energy increases. If there is a high enough imbalance in the energy of the system is high enough, fracturing occurs due to progressive degradation of material strength. The failure process can be therefore broken down into a number of steps based on the level of material degradation and stiffness softening. [7]. Within these steps, crack initiation denotes the stress level in which micro-fracturing is occurring [8]. Crack growth happens at the instance of critical energy release and lasts until when the micro-cracks have joined and the structure can no longer support an increase in the load.

One of the elements appreciably influenced by the material heterogeneity, is the crack initiation angle, in particular for those systems that are subjected to mixed-mode loading conditions [9-11]. In a recent work, Lin and his co-workers [12] proved, with experimental measurements on acoustic emissions of mortar materials, that the crack angle is correlated with the magnitude of the initiation and the failure stresses. The importance of crack initiation angle has also been

recognised by Park and Lange [13], in which a new fracture parameter, named critical crack opening angle, describing the crack opening resistance, has been introduced for cement-based materials. Yang et al. [14] studied the effect of loading type and heterogeneity on the crack geometry, initiation and propagation processes, and concluded that local stresses control crack initiation process, while the loading configuration is responsible for crack inclination and curving. Evangelatos and Spanos [15] used the peridynamic theory to study the effect of the inclination of crack initiation angle on the total energy of a system, estimation of its reliability and its probability of failure.

Another crucial material property, influencing crack initiation and propagation process, is fracture toughness, which represents the critical stress intensity factor (SIF) at crack tip, that can introduce catastrophic crack growth. Fracture toughness is a function of applied loading, crack size and structural geometry, and it is representative of the level of "stress" at the tip of the crack [11]. A high value of fracture toughness makes materials resistant to catastrophic crack extension; alternatively, it may be considered as requiring a large amount of strain energy to create new surfaces.

An accurate and rigorous evaluation of fracture toughness is therefore indispensable for application of fracture mechanics methods in structural integrity assessment. The American Society for Testing and Materials (ASTM) provides standard terminology and formulations with regards to experimental measurements of fracture toughness [16-17]. In parallel with the experimental methods, closed form solutions for analytical calculation of fracture toughness, for determined geometries and loading configurations, have also been developed, and they are expressed as linear combination of SIFs for different crack opening modes [18-24].

If for a given problem that has to be examined, no experimental measurement of fracture toughness is conducted, often values for fracture toughness are chosen from the literature. However, not necessarily a specific value can be used for specific case studies, as fracture toughness depends not only on the constituents of the material, but also on other factors such as geometrical configurations and loading conditions. This assumption may therefore lead to erroneous results and, possibly, to an overestimation of the material resistance.

One of the analytical criteria, which is most frequently used for investigating mixed mode fracture toughness, is the maximum tangential stress (MTS) criterion, where fracture toughness is explicitly expressed as a function of mode I and II SIFs and of the crack initiation angle. Several studies (e.g. [25-26]) revealed that this method, which considers the tangential stresses in the vicinity of the crack tip, especially in the case of mixed mode fracture may not provide reliable values of fracture toughness. Ayatollahi and Aliha [25], for example, conducted a

detailed study on this matter, reporting experimental values of fracture toughness of four different types of rock materials and comparing them with the analytical results from the MTS method; they showed that if the effect of a non-singular stress term, called *T*-stress, is considered, then a better agreement between analytical and experimental results can be achieved. This modified criterion, called generalised maximum tangential stress (GMTS) method, has been applied for several specimens subjected to mixed-mode loading, but none of them includes the effect of material heterogeneity in the calculation of the fracture toughness. The aim of this study is therefore to extend and implement the definition of the GMTS criterion for materials with heterogeneous structure.

The computational framework used in this study for extracting a probabilistic distribution of the crack initiation angle, employs a phase-field formulation [27], in which the initiation and evolution of crack are described by a scalar damage variable assuming values in the range (0,1), where 1 means sound material, and 0 means totally broken material. The non-local analysis of the damage field evolution in an area in proximity of the crack initiation point allows to determine in which direction crack is most likely to propagate. Crack propagation direction is predicted using a probabilistic approach which includes a linear combination of different Probability Density Functions (PDF) of crack initiation angle.

Finally, in the context of stochastic modelling, energy release rate is defined as a function of the randomly variable fracture toughness and a probabilistic distribution of the damage initiation in the fracturing body is sought. Therefore, the damage state in proximity of the crack initiation point is considered to define realistic values of fracture toughness, which is a function of initial crack angle, loading condition and geometry. A probabilistic distribution for crack propagation direction is then defined and used for sampling the angle and calculating fracture toughness for the heterogeneous materials.

The main advantage of the method proposed in this work is the possibility to simply and practically quantify the uncertainty in the fracture toughness value evaluation as a function of other mechanical properties of the material which are directly introduced in a phase-field theory based framework for crack propagation. The material length scale, representative of the size of the damage zone, contributes in defining the degree of heterogeneity of the material. In this way, the statistical information (mean value, standard deviation and correlation length) needed for sampling random values for crack initiation angle will be automatically provided by the numerical simulations using the phase-field theory. Furthermore, it will be proved that the non-Gaussian nature of the fracture toughness and fracture energy can be automatically captured with this method using a Gaussian approach for the crack initiation angle, without the need to

any translation function for sampling random values of these material properties [4-5].

2. Fracture advancement methodology and damage state of the body

In this section, the basic ingredients of the phase-field model used to determine the initiation and propagation of fracture are presented. The variational model proposed in [27-28] is considered, where smeared fracture in an elastic body Ω is described by means of a scalar damage field s, which assumes values in the range (0, 1); when $s = 1$ the material is sound, and, when $s = 0$, it is totally damaged. The internal energy assigned to Ω is

$$E(\mathbf{u}, s) = \int_{\Omega} \left\{ k\frac{1}{2}\,\mathrm{tr}^{-}(\nabla\mathbf{u})^2 + s^2\left[k\frac{1}{2}\,\mathrm{tr}^{+}(\nabla\mathbf{u})^2 + \mu\left(\nabla\mathbf{u}^{\mathbf{2}} - \frac{2}{3}\mathrm{tr}(\nabla\mathbf{u})^2\right)\right]\right\} dx + \frac{G_f}{2}\int_{\Omega}\left(\varepsilon\nabla s^{\mathbf{2}} + \frac{(1-s)^{\mathbf{2}}}{\varepsilon}\right) dx \tag{1}$$

which depends on the displacement field $\mathbf{u}$ and on the damage s. The first integral in Eq. (1) represents the bulk energy, where $k = \lambda + 2\mu/3$ is the bulk modulus, μ and λ are the Lame's coefficients, and the decomposition $\mathrm{tr}^{+}(\nabla\mathbf{u}) = \max\{\mathrm{tr}(\nabla\mathbf{u}), 0\}$ and $\mathrm{tr}^{-}(\nabla\mathbf{u}) = \{\mathrm{tr}(\nabla\mathbf{u}), 0\}$ in positive and negative parts of the trace of $\nabla\mathbf{u}$ is used. The second integral is the fracture energy, which is the sum of a local and a non-local contributions. G_f is the unit fracture energy, and ε is an internal length associated to damage non-locality. The length ε is related to the size of the process zone, as discussed in the following. The energy (1) is minimised under the irreversibility condition $\dot{s} \leq 0$, introduced to forbid material self-healing.

By using the energy (1), different fracture processes are reproduced when tensile or compressive loadings are applied. Indeed, in regions of Ω subjected to tensile states, where volume changes are positive, the opening and evolution of brittle fractures are allowed; while, in compressed regions, where volume changes are negative, cracks are partially forbidden, and only shear fractures can develop, when shear stresses are generated by compressive loadings.

When a fracture forms, the damage parameter s assumes the value $s = 0$ on the fracture surface, and it increases by moving away from that surface. The optimal profile of s in the direction normal to the fracture surface was determined in [29], and its expression is

$$s(x) = 1 - \mathrm{e}^{-\frac{|x-x_0|}{\varepsilon}}, \tag{2}$$

where x is the coordinate in the direction normal to the surface, and x_0 is the intersection point between the normal axis and the surface. From Eq. (2), at distances larger than 2.5ε from the surface ($|x\text{-}x_0| > 2.5\varepsilon$), damage attains values $s > 0.9$, and the material can be considered practically sound. Thus the damaged band around the fracture surface has a thickness of about 5ε, which represents the size of the process zone.

The functional (1) is numerically minimised by using the incremental procedure first proposed in [30], and described in the following. We denote with t the loading parameter of the problem (load or displacement applied on a portion of the body boundary), which is monotonically increased from 0 by means of finite increments. At each loading step, an iterative procedure is performed. Let $(\mathbf{u}_{i-1},s_{i-1})$ be the solution at the (i-1)th loading step, the pair $(\mathbf{u}_i,s_i)$ at the ith step is evaluated by solving the iterative double minimisation procedure shown below.

1. *Initiation*. Set $(\mathbf{u}_i^0, s_i^0)=(\mathbf{u}_{i-1},s_{i-1})$
2. *Iteration j*. For given $(\mathbf{u}_i^{j-1}, s_i^{j-1})$
    - *i.* compute $\mathbf{u}_i^j$ by minimizing $E(\cdot, s_i^{j-1})$
    - *ii.* compute s_i^j by minimizing $E(\mathbf{u}_i^j, \cdot)$
    - *iii.* *Irreversibility condition*: set $s_i^j(x)=\min\{ s_i^j(x) , s_{i-1}(x)\}$, $x\in\Omega$
3. Iterate step 2 until $| s_i^j - s_i^{j-1}|_{L\infty}<s_{max}$, with s_{max} being a fixed tolerance.

At the step $i = 0$ it is set that $(\mathbf{u}_0,s_0) = (\mathbf{0},1)$, so the body is assumed undeformed and uncracked in the initial configuration.

The minimizations at steps *i*. and *ii*. are performed by finding the stationarity point of (1), keeping s and $\mathbf{u}$ fixed, respectively. The corresponding problems are linear elliptic and solutions are numerically found by means of the finite element method. Within the Matlab environment, an in-house code is developed based on triangular elements with affine shape functions. To improve the accuracy in the determination of the field s, the program includes a mesh refinement algorithm, which automatically subdivides those elements at which the values of s become smaller than a given threshold. As a result, within each loading step, in the algorithm an iterative macro-scheme, which includes the process described above, allows for the mesh refinement. While the convergence of the developed algorithm has not been proven theoretically, however the numerical experiments show a fast convergence.

In the next sections, two dimensional simulations are performed by assuming the hypothesis of plane strain state.

3. Fracture toughness calculation: the GMTS criterion

In the context of linear elastic fracture mechanics, elastic stresses in proximity of the crack tip can be written as linear combinatio of angular functions expanded according to infinite series [25]. Based on the GMTS criterion, for a brittle material, crack propagates radially and perpendicular to the direction of maximum tangential stress; the crack initiation point is where the tangential stress $\sigma_{\theta\theta}$ reaches its critical value, and along this direction crack initiates at r_c defined as the critical distance from the crack tip. It is considered that r_c is a constant material property; it is usually considered to be equal to the radius of the process zone. Several methods, both experimental and numerical, have been proposed to estimate the size of this zone for brittle materials [25, 31]. In this work, r_c is considered to be compatible with the size of the process zone estimated on the basis of the theory discussed in the Section 2, therefore, equal to 5ε. Formulation of the tangential stress in the vicinity of crack tip is therefore explicitly given as series expansion in [25] as

$$\sigma_{\theta\theta} = \frac{1}{\sqrt{2\pi r}}\cos\frac{\theta}{2}\left[K_I\cos^2\frac{\theta}{2} - \frac{3}{2}K_{II}\sin\theta\right] + T\sin^2\theta + O(\sqrt{r}) \tag{3}$$

where r and θ are the polar coordinates of a point with respect to the crack tip, K_I and K_{II} are the SIFs for mode I and II respectively and T is the T-stress, which is a constant term defining the stress parallel to the crack and independent of r, the higher order term $O(\sqrt{r})$ of the expansion can be neglected in proximity of the crack tip.

Recalling that crack initiates and propagates in the direction of maximum tangential stress, the crack initiation angle θ_0 (angle that indicates the direction with respect to the direction of the initial notch, where the maximum stresses are found) can be calculated by imposing the condition

$$\left.\frac{\partial\sigma_{\theta\theta}}{\partial\theta}\right|_{\theta=\theta_0} = 0. \tag{4}$$

The calculated angle is used for obtaining the value of the fracture toughness of mixed-mode fracture. Brittle failure happens when $\sigma_{\theta\theta}$ reaches its critical value $\sigma_{\theta\theta c}$. This condition

provides the following expression [25]

$$\sqrt{2\pi r_c}\,\sigma_{\theta\theta c} = \cos\frac{\theta_0}{2}\left[K_I\cos^2\frac{\theta_0}{2} - \frac{3}{2}K_{II}\sin\theta_0\right] + T\sin^2\theta_0. \quad (5)$$

If now the pure mode-I fracture case is considered, K_{II}, T and θ_0 all become equal to zero. Therefore, when fracture occurs K_I reaches its critical value K_{Ic} which corresponds to the mode-I fracture toughness

$$\sqrt{2\pi r_c}\,\sigma_{\theta\theta c} = K_{Ic}. \quad (6)$$

Eq. (5) can be rewritten using Eq. (6) to obtain the value for fracture toughness K_{Ic}

$$K_{Ic} = \cos\frac{\theta_0}{2}\left[K_I\cos^2\frac{\theta_0}{2} - \frac{3}{2}K_{II}\sin\theta_0\right] + T\sin^2\theta_0. \quad (7)$$

The expression in Eq. (7) represents the final form of the GMTS criterion. Closed form solutions for K_I , K_{II} and T have been calculated for defined geometries and loading configurations [25-26, 32-37].

General expression for K_I and K_{II} takes the general form

$$K_I = \sigma^*\sqrt{\pi a}\,F_I\left(\frac{a}{W}\right) \quad (8)$$

$$K_{II} = \sigma^*\sqrt{\pi a}\,F_{II}\left(\frac{a}{W}\right), \quad (9)$$

where σ^* represents the stress field in correspondence of the crack tip, a provides information about the position and the length of the crack, W is a measure of the body geometry, $F_I\left(\frac{a}{W}\right)$ and $F_{II}\left(\frac{a}{W}\right)$ are dimensionless functions of the geometry of the notched body and of the experimental setup. For calculating the values for T, one of the most common methods is based on its calculation from finite element analysis as shown by Ayatollahi et al. [26].

4. Uncertainty quantification: the spectral representation method

In this work, uncertainty is included in the model by sampling random values of θ_0 using the

spectral representation method. With this method, a stochastic field of a two dimensional problem is expressed as [5]

$$\theta_g^{(i)}(x,y) = \theta_0 + \sqrt{2}\sum_{n_1=0}^{N_1-1}\sum_{n_2=0}^{N_2-1}[A_{n_1n_2}^{(1)}\cos\left(\kappa_{1n_1}x + \kappa_{2n_2}y + \phi_{n_1n_2}^{(1)(i)}\right) + A_{n_1n_2}^{(2)}\cos(\kappa_{1n_1}x - \kappa_{2n_2}y + \phi_{n_1n_2}^{(2)(i)})] \quad (10)$$

where $\phi_{n_1n_2}^{(1)(i)}$ and $\phi_{n_1n_2}^{(2)(i)}$ are the realisation for the i_{th} simulation of the independent random phase angles which follow a uniform distribution. Furthermore,

$$A_{n_1n_2}^{(1)} = \sqrt{2S_{gg}(\kappa_{1n_1},\kappa_{2n_2})\Delta\kappa_1\Delta\kappa_2} \quad (11a)$$

$$A_{n_1n_2}^{(2)} = \sqrt{2S_{gg}(\kappa_{1n_1},-\kappa_{2n_2})\Delta\kappa_1\Delta\kappa_2} \quad (11b)$$

$$\kappa_{1n_1} = n_1\Delta\kappa_1 \quad (12a)$$

$$\kappa_{2n_2} = n_2\Delta\kappa_2 \quad (12b)$$

$$\Delta\kappa_1 = \kappa_{1u}/N_1 \quad (13a)$$

$$\Delta\kappa_2 = \kappa_{2u}/N_2 \quad (13b)$$

with

$$n_1 = 0,1,\dots,N_1-1; \qquad n_2 = 0,1,\dots,N_2-1. \quad (14)$$

N_1 and N_2 are the number of intervals where the wave number axes are split, κ_{1u} and κ_{2u} are defined as the upper cut-off wave numbers defining the active region of the spectral density function (SDF) S_{gg}. Therefore, the effect of S_{gg} is operative only for the range

$$-\kappa_{1u} \le \kappa_1 \le \kappa_{1u} \quad \text{and} \quad -\kappa_{2u} \le \kappa_2 \le \kappa_{2u}; \quad (15)$$

outside of this range, S_{gg} is assumed to be equal to 0.

In this work, the SDF takes the form of [5]

$$S_{gg} = \sigma_g^2 \frac{b_1 b_2}{4\pi} \exp\left[-\frac{1}{4}(b_1^2\kappa_1^2 + b_2^2\kappa_2^2)\right] \quad (16)$$

where σ_g is the standard deviation of the field, while b_1 and b_2 represent the correlation length along the two dimensions.

5. PDF of the crack initiation angle θ_0

The uncertainty in the material behaviour is related to heterogeneity of the materials strength that is modelled by defining a random distribution of damage inside of simulation domain. Therefore, similar to the work presented by Gutierrez and de Borst [45], damage parameter instead of material stiffness or fracture energy has been selected as a random parameter. However, due to lack of experimental data and information about the statistics of damage distribution throughout of the material, a computational model has been used to generate a hypothetical possible spatially random field for damage parameters associated to materials with different micro-structure and length scales. The random distribution of damage parameter is linked with the material length scale and particle size distribution (as an index of material heterogeneity) through specifying several threshold values for $\bar{s}$. This aspect also overcomes the issue of the mesh dependency, as the size of the mesh is directly connected to the material length scale as shown in Section 6 in the definition of the parameters for Eq. (1). Different threshold values for damage parameter $\bar{s}$ have been selected in a way to take into account both the influence of distribution of imperfection in the whole specimen and the possible variations in the size of the specimens. Without this, the approach would not be non-local, as it would consider only the damage in proximity of the crack tip.

Therefore, for a given body discretised in finite elements and for a given crack initiation point, positions of the finite element nodes with respect to the crack tip and associated values of *s* are considered. In order to accurately take into account the contribution of the damage state of the body in the definition of θ_0, the so-called fracture process zone (FPZ) should be adequately identified. The FPZ can be identified numerically with the phase-field theory described above. In fact, the damage will spread from the crack tip at a distance which will be included within typical FPZs identified by several works [25, 38-39].

The values for damage in each node provide information about the direction that the crack is most likely to initiate and propagate: in particular, it is likely that the crack spreads through those nodes with a lower value of damage. Therefore, the degree of damage that develops in the body is considered in the procedure formed by the following steps:

1. Calculate the values for damage parameter by using the iterative procedure described in Section 2;
2. For different threshold values $\bar{s}$, select the nodes with $s \leq \bar{s}$;
3. Calculate the polar coordinates with respect to the crack tip of the nodes selected in step 2;
4. Estimate mean value of θ_0 for each threshold value $\bar{s}$;
5. Calculate the overall mean value and the standard deviation of θ_0 from the values estimated in step 4 for each $\bar{s}$;
6. Sample values of θ_0 using the spectral method described in Section 4 and calculate the corresponding values of K_{Ic} using Eq. (7).

Through this method, θ_0 becomes the parameter with stochastic nature and can be then expressed as a vector $\boldsymbol{\theta}_{0g} = [\theta_g^{(1)}, \theta_g^{(2)}, \dots, \theta_g^{(n_{FE})}]$, with n_{FE} being the number of elements forming the finite element mesh that discretises the problem under investigation. Therefore, the probabilistic generalised maximum tangential stress (PGMTS) criterion can be achieved in terms of θ_{0g} using Eq. (7) as

$$\boldsymbol{K_{Ic}}(\boldsymbol{\theta}_{0g}) = \cos\frac{\boldsymbol{\theta}_{0g}}{2}\left[K_I \cos^2\frac{\boldsymbol{\theta}_{0g}}{2} - \frac{3}{2}K_{II}\sin\boldsymbol{\theta}_{0g}\right] + T\sin^2\boldsymbol{\theta}_{0g}\,. \tag{17}$$

Finally, fracture energy G_f can also be calculated using the elastic crack-tip solution and a simple relationship between K_{Ic} and G_f as [40]:

$$\frac{K_{Ic}^2}{E'} = G_f, \tag{18}$$

which is developed based on the theories of Griffith [7]. In the Eq. 18, $E' = E$ for the plane stress conditions, and $E' = E/(1-\nu^2)$ for the plane strain conditions with E being Young's modulus and ν Poisson's ratio.

6. Numerical analyses and discussion of the results

6.1. Notched concrete slab

In order to verify the proposed methodology, the first example considered in this study is a finite element model of a concrete slab with size of 500 mm x 400 mm (see Fig. 1). This example was also simulated by Huang et al. [41]. Young's modulus E and Poisson's ratio ν are chosen equal to 25000 N/mm^2 and 0.18 respectively. An initial deterministic value for G_f equal to 0.15 N/mm is assigned to the model [3]. A value of $\varepsilon = 8$ mm is selected, while the size of the mesh is chosen to be equal to 8 mm. The value for ε is chosen, following the considerations listed in [29], on the basis of the average size of the material constituents; in particular, ε is typically assumed to be 2-3 times the characteristic material length scale. As concrete is formed by constituents of different sizes, an average dimension of 4-5 mm is here considered and, consequently, the value of 8 mm for ε is selected. An initial crack of dimension 4 x 40 mm is modelled in the middle of the specimen. In order to create a typical mixed mode crack condition, the inclination of the crack with respect to the distributed load is set to be 45º. The simulation is performed in quasi-static displacement-controlled condition.

In order to calculate K_{Ic} using Eq. (7), the value of r_c has been selected according to the recommendations proposed in [25 and 38-39]. In [25] r_c is calculated for the brittle materials as a function of K_{Ic} and a range of values between 45 and 60 N/mm$^{3/2}$ was assumed for K_{Ic}, which gives a range of values between 35 and 45 mm for r_c, approximately. In [38] and [39] a combination of analytical and experimental investigations on concrete specimens subjected to both pure mode-I and mixed-mode loading provided a range of values for the size of FPZ, which vary from a minimum of 40 up to a maximum of 140 mm. Therefore, the value of r_c for this example is chosen equal to 40 mm which is within the range proposed in the literature.

For this specific example, the explicit formulation of Eq. (8) and (9) are expressed, together with the explicit expression for T, as [32]

$$K_I = \sigma\sqrt{\pi a}\sin^2\beta \tag{19a}$$

$$K_{II} = \sigma\sqrt{\pi a}\sin\beta\cos\beta \tag{19b}$$

$$T = \sigma\cos 2\beta \tag{19c}$$

where, σ is applied stress to the body, a is half length of the initial notch, and β is inclination angle of the notch with respect to the loading direction. For this example σ = 8.6 N/mm^2, a = 20 mm and β = 45º [41].

Fig. 2 shows the evolution of the damage in proximity of the crack tip that has been taken into account to generate PDFs of θ_0. For simplicity, only the upper half of the specimen is considered and presented in Fig. 2. The area where the damage spreads, is smaller than the size of FPZ considered in literature [38-39], which vary from a minimum of 40 mm up to a maximum of 140 mm for pure mode I failure.

Table 1 summarizes the values obtained for crack initiation angle with respect to the direction of the notch, considering different values of $\bar{s}$ together with the calculated mean value and standard deviation. In order to validate the result, the mean value is compared with the results from literature [41] and with the value calculated considering the condition [25]

$$[K_I \sin\theta_0 + K_{II}\,(3\cos\theta_0 - 1)] - \frac{16}{3} T\sqrt{2\pi r_c}\cos\theta_0 \sin\frac{\theta_0}{2} = 0 \tag{20}$$

which is the explicit form of Eq. (4). For this example, Huang et al. [41] provided a value for crack initiation angle equal to 53.1º, while the result obtained using Eq. (20) is 52.7º. The summary of all the results can be found in Table 1. It can be observed that the value reported in [41] and the value calculated through the methodology proposed in this work differ about 4º.

The mean value and standard deviation shown in Table 1 are then considered as an estimate to sample random values for θ_0 using the Gaussian process shown in Eq. (10).

In the first instance, a deterministic value of the fracture toughness is calculated using Eq. (7) and the mean value of θ_0. The fracture toughness is therefore equal to 60.9 N/mm$^{3/2}$. Griffith's Energy G_f is then calculated as G_f = 0.14 N/mm, consistent with the range of values of G_f for concrete found in literature [3, 42].

This example is one of those used in literature to study mixed-mode conditions for the materials. For this reason, this example has been used with the main purpose of comparing the crack initiation angle available in literature with the value crack initiation angle as mean value of the probabilistic distribution obtained.

With regards to the parameters involved in the stochastic approach described in section 4, the number of terms used for the spectral representation series is chosen as $N_1 = N_2 = 20$, the cut-off wave numbers $\kappa_{1u} = \kappa_{2u} = 2\pi$ and $b_1 = b_2 = 1$ [30]. Once the mean value and standard deviation for θ_0 are defined, they are used to sample values of θ_0 according to a Gaussian distribution, as shown in Fig. 3. This sample for θ_0 is then substituted into the expression for K_{Ic} of Eq. (7), and a sample for K_{Ic} is then obtained as shown in Fig. 4. The sample shown has

a mean value of 60.5 N/mm$^{3/2}$. The calculated values of K_{Ic} can finally be used to get a distribution, shown in Fig. 5, of the values for G_f with mean value 0.14 N/mm and standard deviation of approximately 5%. It is worth noting, as shown in the Figs. 4 and 5, that the values of K_{Ic} and G_f don't follow the same Gaussian trend of θ_0, but a non-Gaussian trend. In particular, the probability functions plotted in the Figs. 4 and 5 follow a Weibull distribution. This trend is consistent with the conclusion from several works [3, 5] that heterogeneous distributions of G_f follow a non-Gaussian (either lognormal or Weibull) distributions. This results show that the proposed methodology is capable to automatically capture the non-Gaussian distribution of a given normally-distributed statistical information (e.g. mean value, standard deviation, correlations), using the translation field functions, which satisfy specific constrains and compatibility conditions associated to the related random field [5]. In fact, despite the simplicity of the Gaussian distributions for sampling from simple statistical information, their use for creating a sample of fracture toughness may lead to the generation of negative, and therefore physically meaningless, values. With the method proposed in this work, we will be able to benefit from the simplicity of Gaussian field theory while generating a realistic and physically meaningful distribution for K_{IC}.

6.2 The four-point Single-Edge Notched Shear (SENS) beam

The second example used in this study is the four-point SENS beam studied in [43]. This benchmark is one of the most widely used to validate numerical models for simulating mixed-mode crack propagation in concrete. A wide range of experimental data is available in literature, and a satisfactory crack scatter is available and has been summed up in [44]. Specimen geometry, boundary conditions and material properties about this benchmark are shown in Fig. 6. Young's modulus E is equal to 24800 N/mm^2, and Poisson's ratio is equal to 0.18. Because also for this second case study a concrete specimen is considered, a value for $\varepsilon = 8$ mm is again selected, while the size of the mesh is chosen equal to 5 mm. For the same reason, the values for the parameters involved in the definition of the spectral representation method are chosen as in the previous case study.

For this benchmark, the explicit form of Eq. (8) and (9) for K_I and K_{II} take the form [18]

$$K_I = \frac{F}{BW}\left(1 - \frac{d}{L}\right) F_I \sqrt{\pi a} \tag{21a}$$

$$K_{II} = \frac{F}{BW}\left(1 - \frac{d}{L}\right) F_{II} \sqrt{\pi a} \tag{21b}$$

where F is the force applied to the specimen, and is selected equal to 132.2 kN, B is the specimen thickness equal to 152 mm, W is the specimen height equal to 306 mm, d = 61 mm is the distance from the middle of the specimen of the force applied and the pin , L is half of the total length of the specimen equal to 458 mm and a is the length of the initial notch equal to 82 mm. F_I and F_{II} are geometry functions depending on specimen geometry and their values for these two functions are available in [18]. Value for T is equal to -0.04 N/mm^2, calculated in [35] from Finite Elements analysis. As discussed by Smith et al. [32], T can have negative values.

For this example, from Eq. (21a) and (21b), F_I = -0.1 and F_{II} = 1.12. Mode-I and Mode-II SIFs can be hence calculated and they are equal to -3.9 N/mm$^{3/2}$ and 44.5 N/mm$^{3/2}$. It is worth noticing that Mode-I SIF has also a negative value. This happens when (i) shear-mode is prevalent on opening-mode mechanisms and (ii) crack lips closure prevails over crack opening [35]; therefore, physically this means that mode-I opening mode has a very small influence of the fracturing process. With this regards, Fig. 7 shows the variation of F_I over the variation of the ratio d/W (as d/W increases, the shear failure prevails over opening failure). It can be seen that when d/W decreases, shear effect increases, making the value for F_I smaller, until it disappears for $d/W > 1.5$.

Fig. 8 shows the evolution of damage in proximity of the initial notch, and it is considered for the generation of the mean value and standard deviation of θ_0. As can be seen, also for this case study the area where the damage spreads is compatible with the size of FPZ considered in literature [25, 38-39].

Table 2 summarizes the values of crack initiation angle with respect to the direction of the initial notch, obtained considering different values of $\bar{s}$ together with the calculated mean value and standard deviation.

The obtained mean value of θ_0 is equal to 74.1º with respect to the direction of the initial notch. The value of θ_0 calculated using Eq. (20) is equal to 72.2º, which is in good agreement with the value obtained numerically. As for the previous example, the deterministic values of fracture toughness and fracture energy are first calculated: K_{Ic} is equal to 48.1 N/mm$^{3/2}$ while Griffith's Energy G_f is then calculated as G_f = 0.095 N/mm.

Once the mean value and standard deviation for θ_0 are defined as listed in Table 2, different values of crack initiation angle are sampled using the spectral approach, as shown in Figure 9. This sample is then used together with the expression for K_{Ic} (i.e., Eq. (7)), and a sample for K_{Ic} is then obtained as shown in Fig. 10. The sample has a mean value of 48.22 N/mm$^{3/2}$. The

calculated values of K_{Ic} is finally used to get a distribution of the values for G_f which have mean value of 0.094 N/mm and standard deviation of approximately 4%. It is worth noting, as shown in Figs. 10 and 11, that also for this example K_{Ic} and G_f follow a log-normal trend, consistent with the conclusion from the previous example and from literature [3,5] that heterogeneous distributions of K_{Ic} and G_f follow a non-Gaussian trend.

7. Conclusions

A novel approach for uncertainty quantification of the random fields in the physical domains is presented. The uncertainty in the mechanical properties of the bodies subjected to damage is quantified by considering the damage state developed in the vicinity of the crack initiation points. Distribution of the damage, predicted using a phase-field model capable of reproducing mixed mode loading conditions, is then employed to estimate the mean value and the standard deviation for direction of crack evolution in the body. This statistical information is then used to create samples for the crack initiation angle by means of the Gaussian spectral representation approach. The calculated sample is finally used to calculate spatially-varying values of the fracture toughness, and consequently the fracture energy for the mixed-mode crack propagation conditions. In first instance, a concrete slab with an internal notch with an inclination of 45º and subjected to uniaxial traction is studied. Calculated mean value for the crack initiation angle (57.1º), is in a good agreement with value of the crack initiation angle found in literature (53.1º), with a difference of only 4º. The second example studied is the four-point bending beam, one of the examples most widely used to validate models considering the mixed-mode conditions. Also for this case study, the mean value for the crack initiation direction (74.1º with respect to the direction of the initial notch) is in very good agreement with the value calculated analytically (72.2º). For both examples, the calculated values of the fracture toughness and the fracture energy are in excellent agreement with values from literature. Furthermore, the most interesting aspect of this method is its capability, by using Gaussian-related statistical information, to capture the non-Gaussian nature of the statistical distribution of the fracture toughness and fracture energy for brittle materials.

Acknowledgement
This study was supported by EPSRC UK (No. EP/M506679/1).

References

[1] Geers MG, Kouznetsova VG, Brekelmans WA. Multi-scale computational homogenization: trends and challenges. J Comput Appl Math 234(7), 2010, 2175-2182.
[2] Miehe C, Bayreuther CG. On multiscale FE analyses of heterogeneous structures: from homogenization to multigrid solvers. Int J Numer Methods Eng 71(10), 2007, 1135-1180.
[3] Yang Z, Xu XF. A heterogeneous cohesive model for quasi-brittle materials considering spatially varying random fracture properties. Comput Method Appl M 197(45), 2008, 4027-4039.
[4] Stefanou G. The stochastic finite element method: past, present and future. Comput M Appl M. 198(9), 2009, 1031-1051.
[5] Georgioudakis M, Stefanou G, Papadrakakis M. Stochastic failure analysis of structures with softening materials. Eng Struct 61, 2014, 13-21.
[6] Yang ZJ, Su XT, Chen JF, Liu GH. Monte Carlo simulation of complex cohesive fracture in random heterogeneous quasi-brittle materials. Int J Solids Struct 46(17), 2009, 3222-3234.
[7] Griffith AA. The phenomena of rupture and flow in solids. Philos T Roy Soc A 221, 1921, 163-198.
[8] Eberhardt E, Stead D, Stimpson B, Read RS. Identifying crack initiation and propagation thresholds in brittle rock. Can Geotech J 35(2), 1998, 222-233.
[9] Kim JH, Paulino GH. T-stress, mixed-mode stress intensity factors, and crack initiation angles in functionally graded materials: a unified approach using the interaction integral method. Comput Method Appl Mech 192(11), 2003, 1463-1494.
[10] Li YP, Chen LZ, Wang YH. Experimental research on pre-cracked marble under compression. Int J Solids Struct 42(9), 2005, 2505-2516.
[11] Aliha MR, Ayatollahi MR, Smith DJ, Pavier MJ. Geometry and size effects on fracture trajectory in a limestone rock under mixed mode loading. Eng Fract Mech 77(11), 2010, 2200-2212.
[12] Lin C, Zhu W, Li S, Guo Y, Wen N, Yang L. Influence of 3D-crack angle on strength of mortar material. Yantu Lixue/Rock Soil Mech 27(SUPPL.), 2006, 622-626.
[13] Park CW, Lange DA. Fracture Parameters and Post-Peak Behavior Evaluation under LEFM on Bonded Cement-Based Materials. InKey Engineering Materials. Vol. 324, 2006, 587-590). Trans Tech Publications.
[14] Yang YF, Tang CA, Xia KW. Study on crack curving and branching mechanism in quasi-brittle materials under dynamic biaxial loading. Int J Fract 177(1), 2012, 53-72.
[15] Evangelatos GI, Spanos PD. A collocation approach for spatial discretization of stochastic peridynamic modeling of fracture. J Mech Mater Struct 6(7), 2011, 1171-1195.
[16] ASTM E1823-10a. Standard terminology relating to fatigue and fracture testing, 2011, American Society for Testing and Materials.
[17] ASTM E1820-11. Standard test method for measurement of fracture toughness, 2011, American Society for Testing and Materials.
[18] Fett T. Stress intensity factors and weight functions for special crack problems Vol. 6025, 1998, FZKA.
[19] Chang SH, Lee CI, Jeon S. Measurement of rock fracture toughness under modes I and II and mixed-mode conditions by using disc-type specimens. Eng Geol 66(1), 2002, 79-97.
[20] Aliha MRM, Ayatollahi MR, Kharazi B. Numerical and Experimental Investigations of Mixed Mode Fracture in Granite Using Four-Point-Bend Specimen. Damage Fract Mech 2009,275-283.
[21] He, MY, Hutchinson JW. Asymmetric four-point crack specimen. J Appl Mech 67(1), 2000, 207-209.
[22] Shahani AR, Tabatabaei SA. Computation of mixed mode stress intensity factors in a four-point bend specimen. Appl Math Model 32(7), 2008, 1281-1288.
[23] Lim IL, Johnston IW, Choi SK, Boland JN. Fracture testing of a soft rock with semi-circular specimens under three-point bending. Part 1—mode I. Int J Rock Mech Min 1994, 185-197.
[24] Lim IL, Johnston IW, Choi SK, Boland JN. Fracture testing of a soft rock with semi-circular specimens under three-point bending. Part 2—mixed-mode. Int J Rock Mech Min 1994, 199-212.
[25] Ayatollahi MR, Aliha MR. On the use of Brazilian disc specimen for calculating mixed mode I–II fracture toughness of rock materials. Eng Fract Mech 75(16), 2008, 4631-4641

[26] Ayatollahi MR, Pavier MJ, Smith DJ. Determination of T-stress from finite element analysis for mode I and mixed mode I/II loading. Int J Fract 91(3), 1998, 283-298.
[27] Amor H, Marigo JJ, Maurini C. Regularized formulation of the variational brittle fracture with unilateral contact: numerical experiments. J Mech Phys Solids 57(8), 2009, 1209-1229.
[28] Freddi F, Royer-Carfagni G, Regularized variational theories of fracture: a unified approach. J Mech Phys Solids 58, 2010, 1154–1174.
[29] Lancioni G, Royer-Carfagni G. The variational approach to fracture mechanics. A practical application to the French Panthéon in Paris. J Elast 95(1-2), 2009, 1-30.
[30] Bourdin B, Francfort GA, Marigo JJ. Numerical experiment in revisited brittle fracture. J Mech Phys Solids 48, 2000, 797-826.
[31] Schmidt RA. A microcrack model and its significance to hydraulic fracturing and fracture toughness testing. The 21st US Symposium on Rock Mechanics (USRMS), 1980, American Rock Mechanics Association.
[32] Smith DJ, Ayatollahi MR, Pavier MJ. The role of T- stress in brittle fracture for linear elastic materials under mixed- mode loading. Fatigue Fract Eng M 24(2), 2001, 137-150.
[33] Fett T. Stress Intensity Factors, T-stresses, Weight Functions: Supplement Volume, 2009, KIT Scientific Publishing.
[34] Ayatollahi MR, Aliha MRM. Wide range data for crack tip parameters in two disc-type specimens under mixed mode loading. Comp Mater Sci 38(4), 2007, 660-670.
[35] Ayatollahi MR, Aliha MRM. On the use of an anti- symmetric four- point bend specimen for mode II fracture experiments. Fatigue Fract Eng M. 2011,34.11:898-907.
[36] Ayatollahi MR, Aliha MRM. Fracture toughness study for a brittle rock subjected to mixed mode I/II loading. Int J Rock Mech Min 44(4), 2007, 617-624.
[37] Ayatollahi MR, Aliha MRM. Mixed mode fracture analysis of polycrystalline graphite–a modified MTS criterion. Carbon 46(10), 2008, 1302-1308.
[38] Dong W, Wu Z, Zhou X, Dong L, Kastiukas G. FPZ evolution of mixed mode fracture in concrete: experimental and numerical. Eng Fail Anal 75, 2017, 54-70.
[39] Yao W, Wu KR, Li ZJ. Fracture process zone of composite materials as concrete. Third International Conference on Fracture Mechanics of Concrete and Concrete Structures(FRAMCOS-3). 1998.
[40] Irwin GR. Analysis of stresses and strains near the end of a crack traversing a plate. Spie Milestone Ser MS 137(167-170), 1997, 16.
[41] Huang D, Lu G, Liu Y. Nonlocal Peridynamic Modeling and Simulation on Crack Propagation in Concrete Structures. Math Probl Eng 2015, 2015.
[42] Fernández-Canteli A, Castañón L, Nieto B, Lozano M. Determining fracture energy parameters of concrete from the modified compact tension test. Frattura ed Integrità Strutturale 30, 2014, 383.
[43] Arrea M. Mixed-mode crack propagation in mortar and concrete, 1982, Cornell University.
[44] Most T. Stochastic crack growth simulation in reinforced concrete structures by means of coupled finite element and meshless methods. 2005.
[45] Gutierrez M. and de Borst, R. Deterministic and stochastic analysis of size effects and damage evolution in quasi-brittle materials. Arch Appl Mech 69, 1999, 655-676.
[46] Mousavi Nezhad M, Gironacci E, Rezania M, Khalili N. (2017) Stochastic modelling of crack propagation in materials with random properties using isometric mapping for dimensionality reduction of nonlinear data sets. Int J Numer Methods Eng (In Press), 2017.

Figures

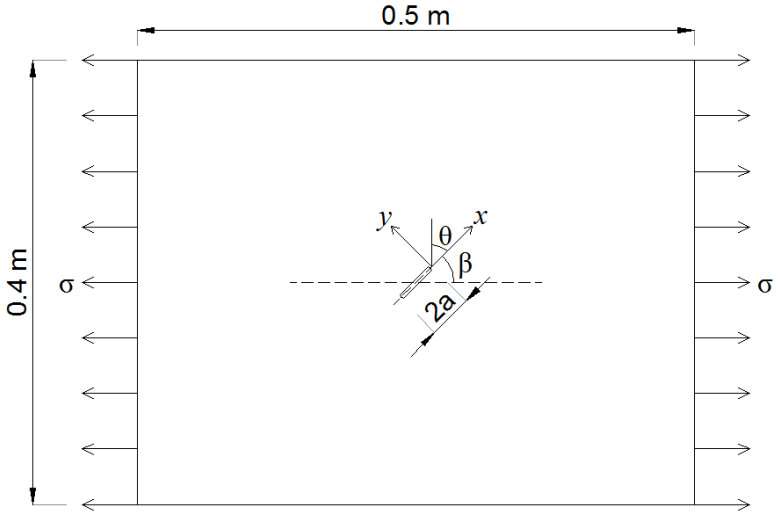

Fig 1. Geometry and loading condition of the considered concrete panel with an inclined central notch.

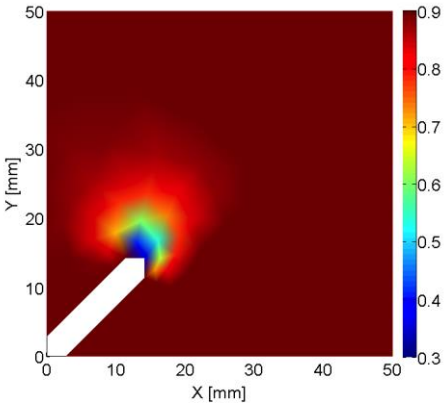

606
607 **Fig 2**. Local area in proximity of the crack tip for the notched concrete panel: the effect of the damage
608 influences the direction of crack initiation considering the damage state at the time step immediately before
609 failure starts.
610

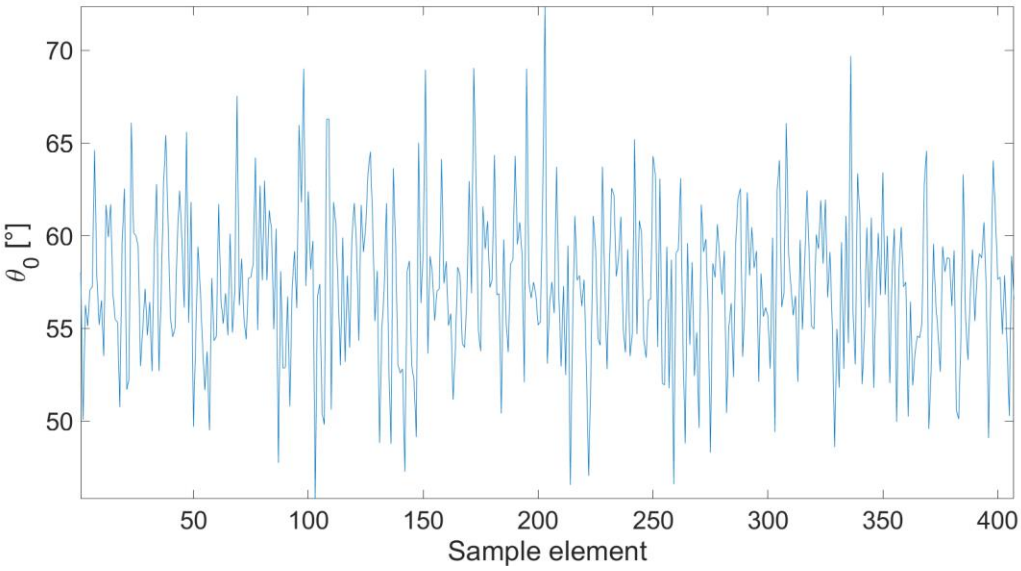

611

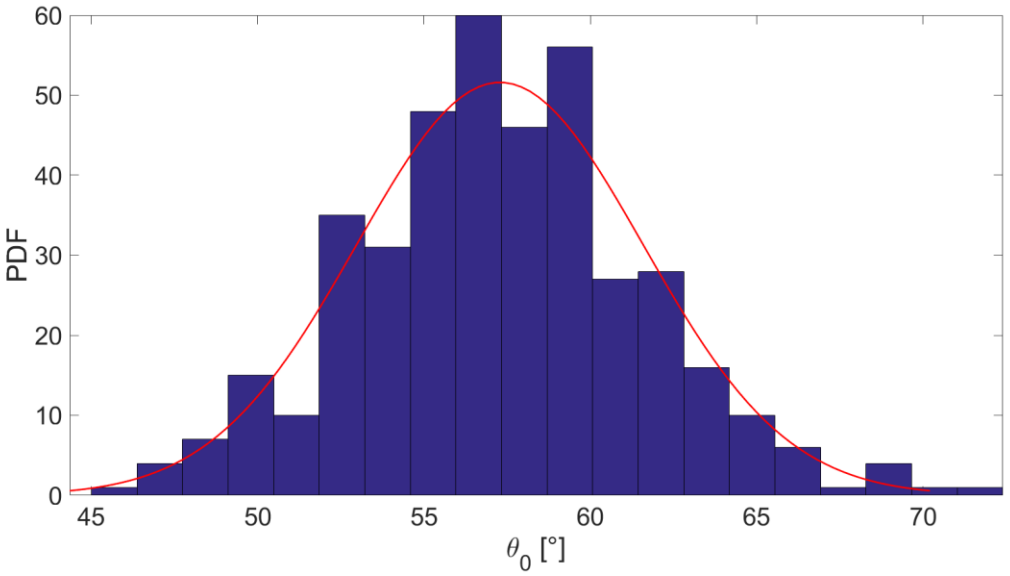

612

Fig 3. Sample for 350 values of θ_0 (top) and PDF with Gaussian nature (bottom). The method shown in Eq. (10) is used to generate each sample.

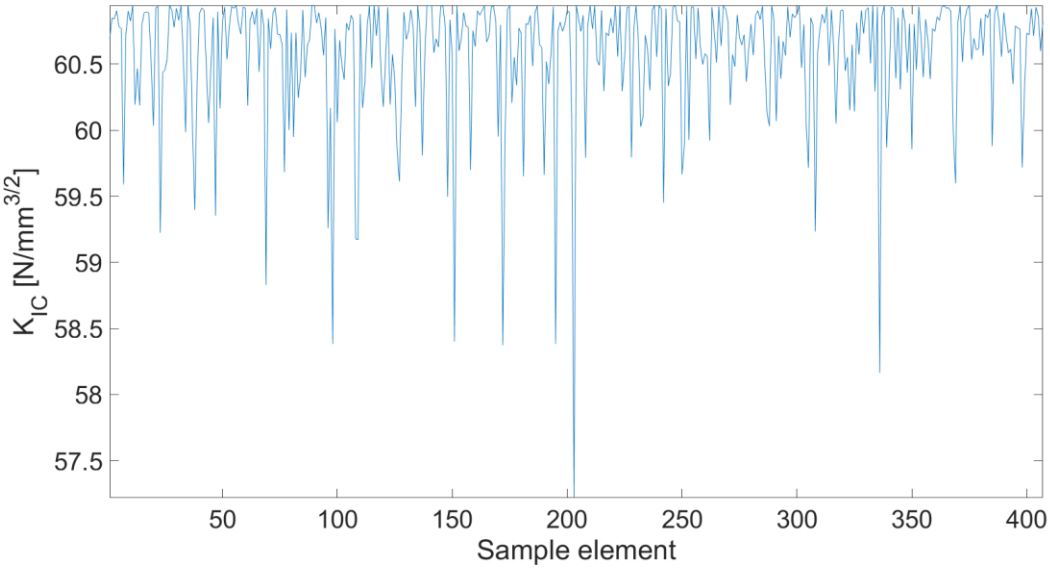

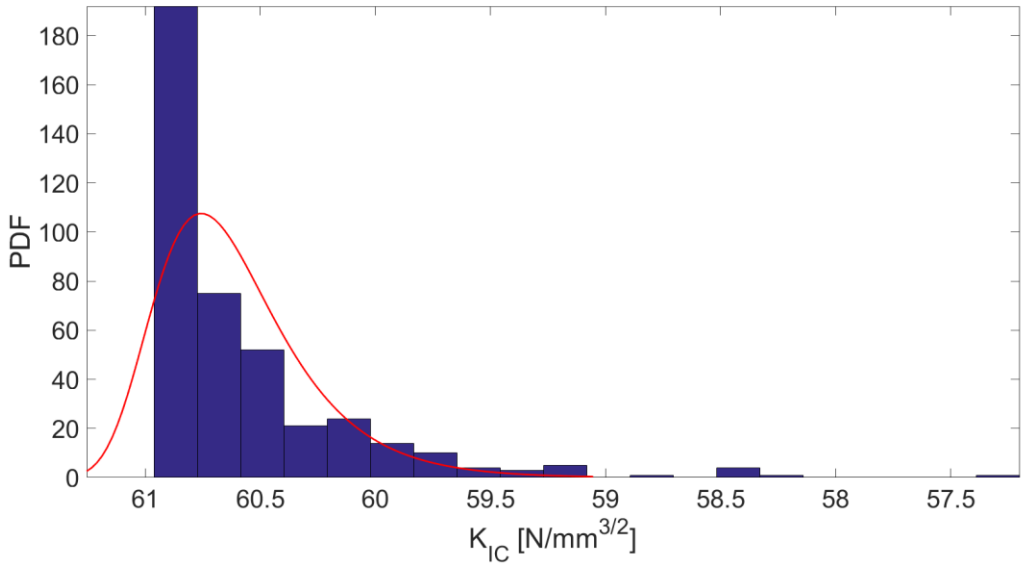

Fig 4. Sample of K_{Ic} generated from the sample of crack initiation angle (top) and relative PDF (bottom): it can be observed that the PDF follows a non-Gaussian distribution, result consistent with assumptions from literature [3-5].

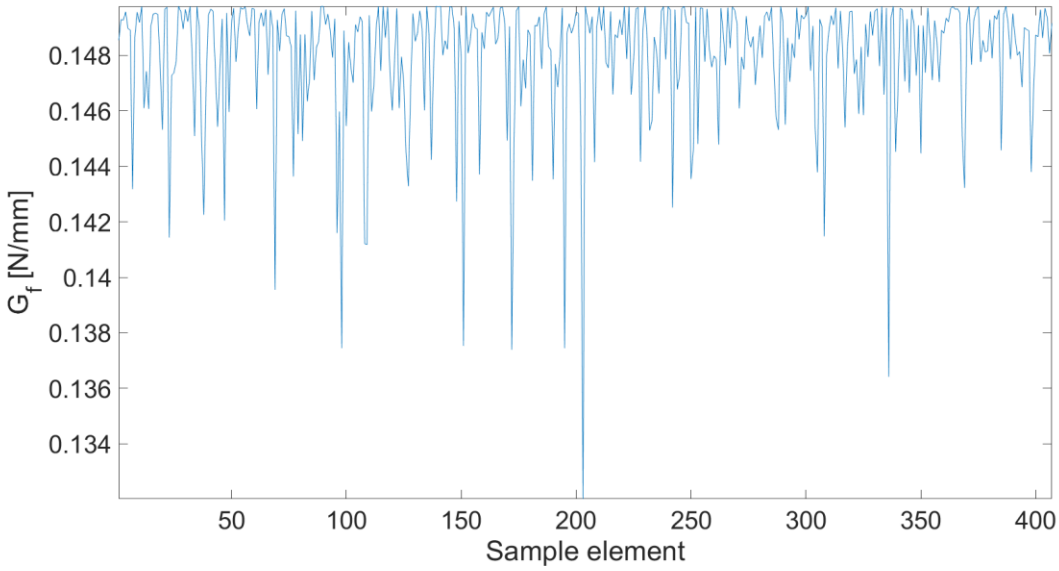

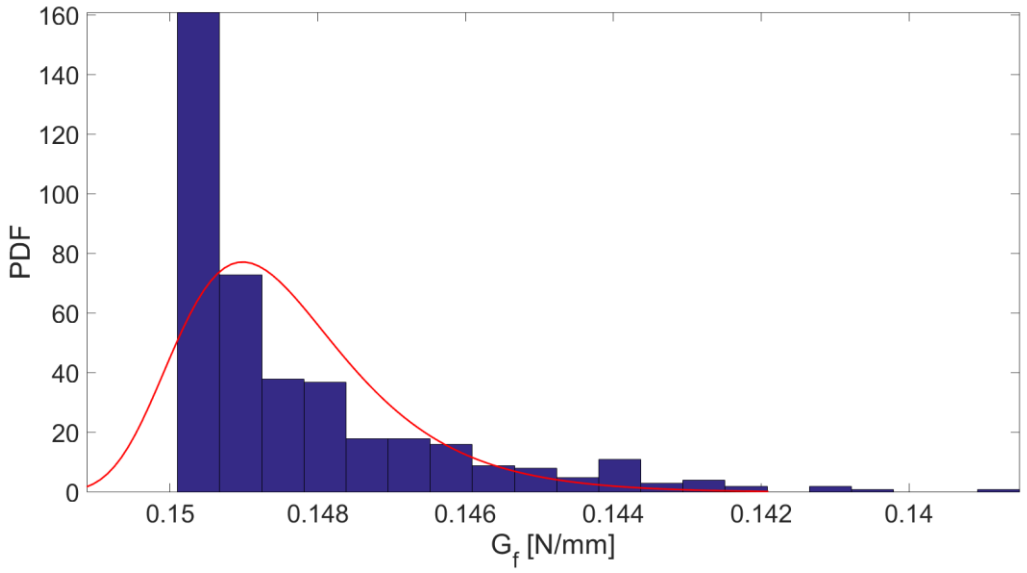

Fig 5. Sample of G_f calculated from K_{Ic} (top) and relative Probabilistic distribution of one sample of G_f: it can be observed that its behaviour follows a lognormal distribution, behaviour consistent with the assumption that non-Gaussian distributions well describe the physical trend of brittle materials such as concrete. [3-5].

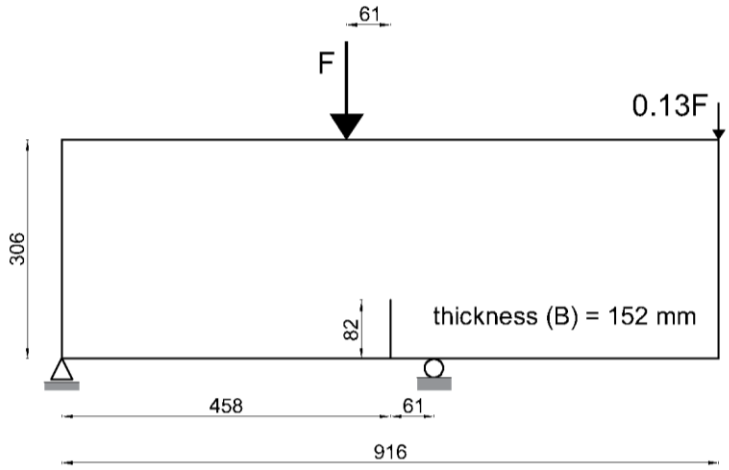

Fig 6. Geometry and load of the SENS beam.

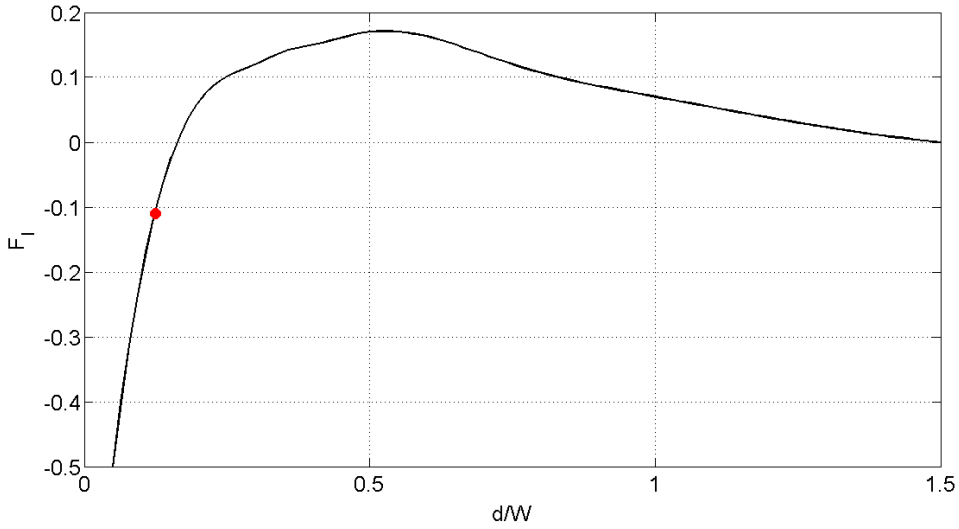

Fig 7. Geometric function F_I trend as function of d/W for L/W = 3.0 and a/W = 0.3. F_I has negative values for small values of d/W, and increases its values for increasing d/W. For larger values (d/W > 1.5) the contribution of mode I component vanishes.

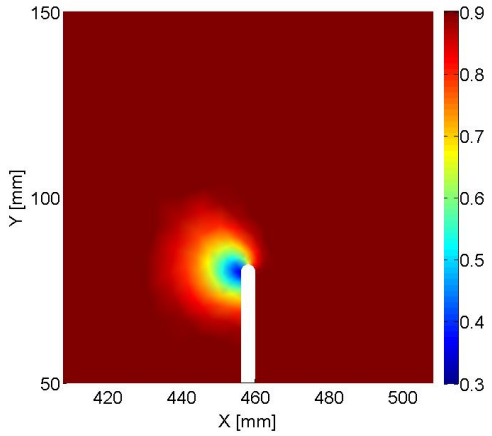

Fig 8. Local area in proximity of the crack tip of the four point SENS beam: the effect of the damage influences also for this example the direction of crack initiation. Nodes closed to the crack tip have a lower value of damage and therefore a higher influence for the determination of the crack initiation angle.

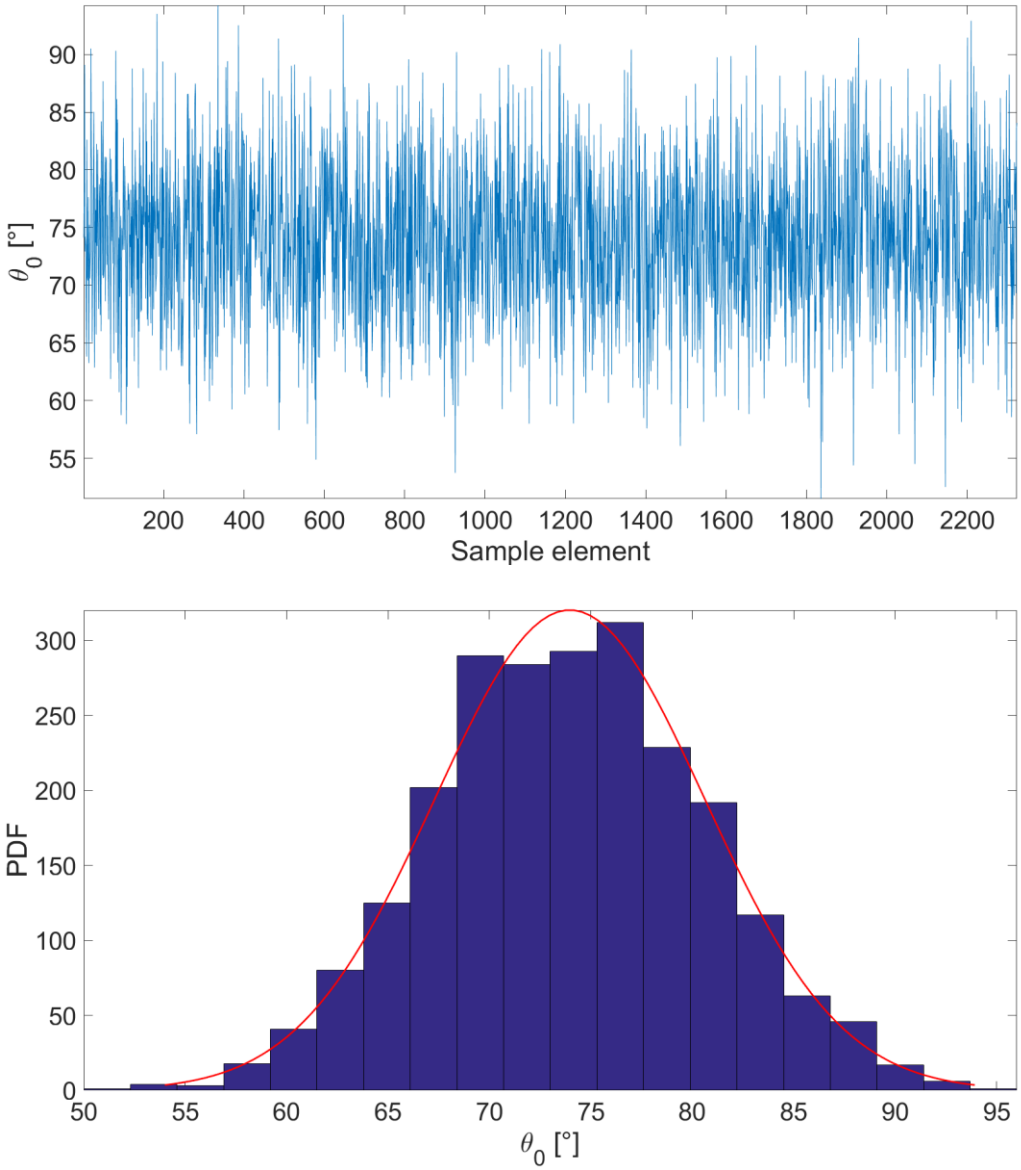

Fig 9. Sample for 2300 values of θ_0 (top) and PDF with Gaussian nature (bottom). The method shown in Eq. (10) is used to generate each sample.

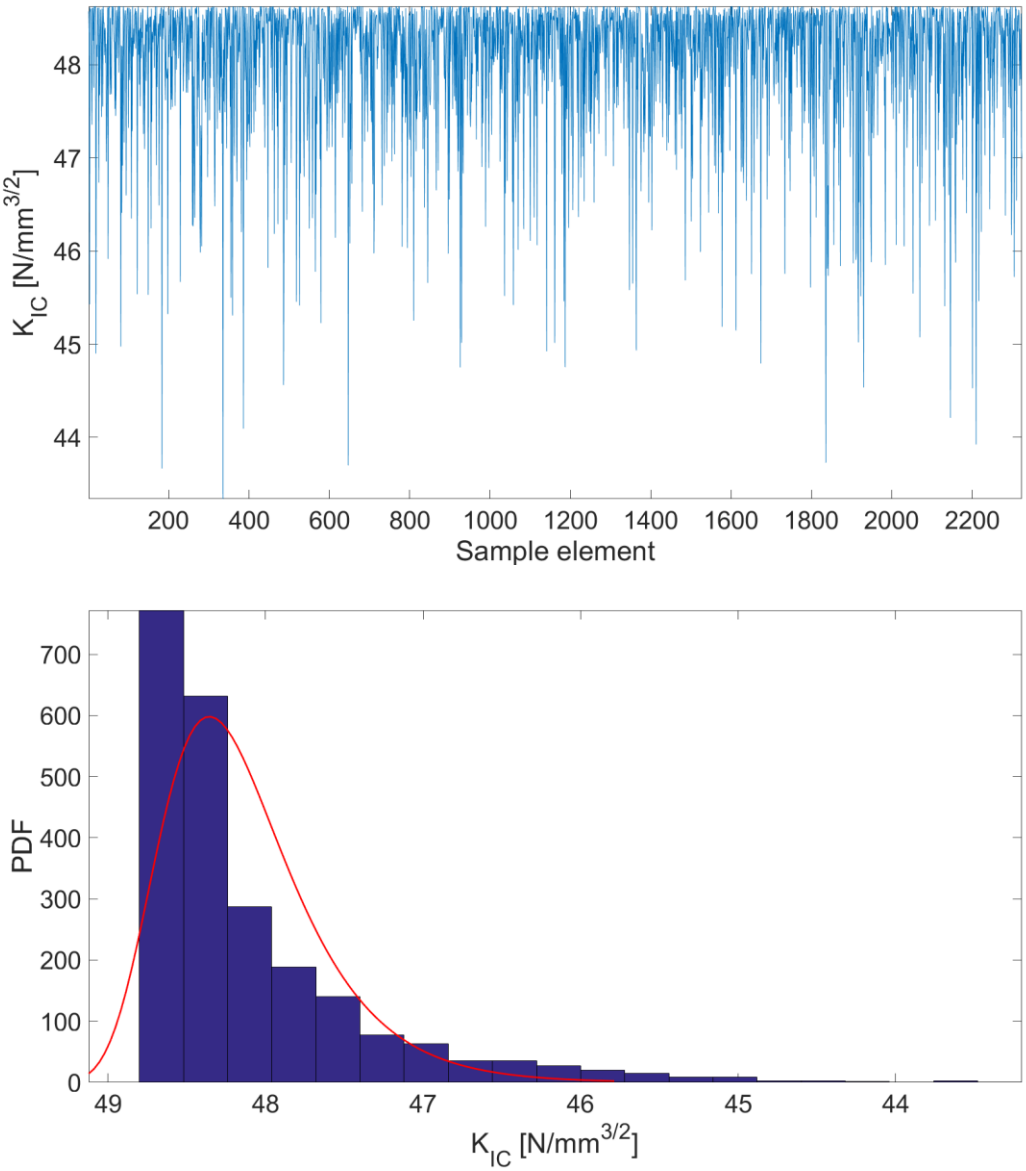

Fig 10. Sample of K_{Ic} generated from the sample of crack initiation angle (top) and relative PDF (bottom): the PDF follows also in this case a non-Gaussian distribution [3-5].

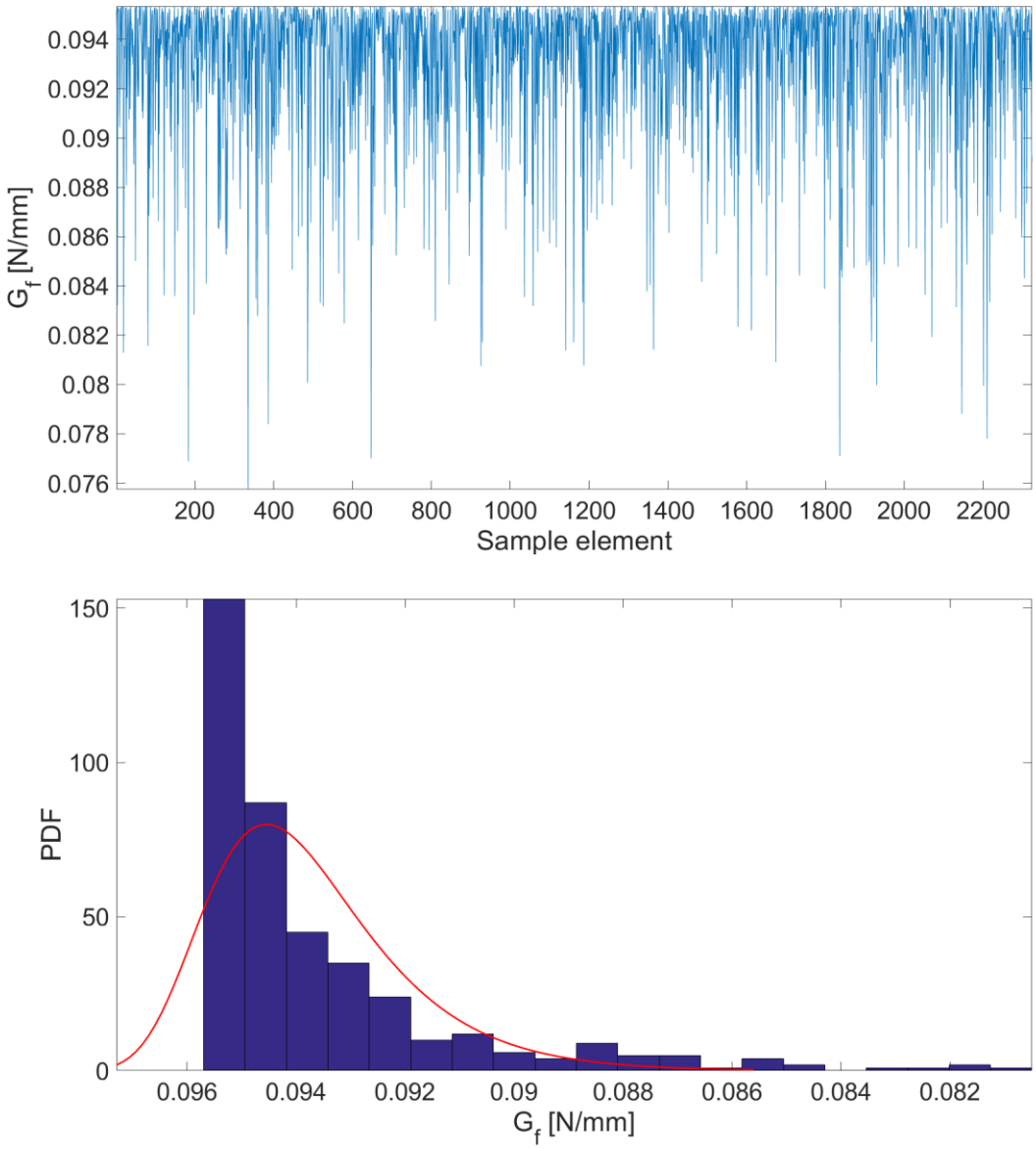

Fig 11. Sample of G_f calculated from K_{Ic} (top) and relative Probabilistic distribution of one sample of G_f: Also in this example its behaviour follows a non-Gaussian trend, behaviour consistent with the assumption that non-Gaussian distributions well describe the physical trend of brittle materials such as concrete. [3-5].

669 **Tables**

670 **Table 1**. Mean values for θ_0 estimated in proximity of the crack tip for different threshold values of $\bar{s}$

$\bar{s}$	**0.4**	**0.5**	**0.6**	**0.7**	**0.8**	**Mean value θ_0**	**Standard deviation**	**Crack initiation angle, [41]**	**Crack initiation angle, Eq (20)**
$\boldsymbol{\theta_0}$	45º	65.3º	60.3º	56.9º	58º	**57.1º**	7.5º	**53.1º**	**52.7º**

671

672

673 **Table 2**. Values for θ_0 estimated in proximity of the crack tip for different threshold values of $\bar{s}$

$\bar{s}$	**0.4**	**0.5**	**0.6**	**0.7**	**0.8**	**Mean value**	**Standard deviation**	**Crack initiation angle, Eq (20)**
$\boldsymbol{\theta_0}$	89.7º	79.6º	72.6º	74.9º	63.6º	**74.1º**	10.8º	**72.2º**

674